

Adsorption mechanism of copper ions on porous chitosan membranes: Equilibrium and XPS study

Azadeh Ghaee^{*1} and Mohammad Mahdi Zerafat²

¹ Department of Life Science Engineering, Faculty of New Sciences & Technologies,
University of Tehran, P.O. Box 14399-55941, Tehran, Iran

² Faculty of Advanced Technologies, Nano Chemical Engineering Department, Shiraz University, Shiraz, Iran

(Received June 06, 2015, Revised September 20, 2016, Accepted September 27, 2016)

Abstract. Heavy metal contamination has attracted considerable attention during recent decades due to the potential risk brought about for human beings and the environment. Several adsorbent materials are utilized for the purification of contaminated water resources among which chitosan is considered as an appropriate alternative. Copper is a heavy metal contaminants found in several industrial wastewaters and its adsorption on porous and macroporous chitosan membranes is investigated in this study. Membranes are prepared by phase inversion and particulate leaching method and their morphology is characterized using SEM analysis. Batch adsorption experiments are performed and it is found that copper adsorption on macroporous chitosan membrane is higher than porous membrane. The iso-steric heat of adsorption was determined by analyzing the variations of temperature to investigate its effect on adsorption characteristics of macroporous chitosan membranes. Furthermore, desorption experiments were studied using NaCl and EDTA as eluants. The mechanism of copper adsorption was also investigated using XPS spectroscopy which confirms simultaneous occurrence of chelation and electrostatic adsorption mechanisms.

Keywords: macroporous chitosan membrane; adsorption; desorption; isotherm; XPS study

1. Introduction

Heavy metal contamination of water resources has attracted considerable attention in recent decades due to its potential ecological risks to plants, animals and microorganisms as well as carcinogenic risks to human beings. Copper is a key constituent of many enzymes catalyzing oxidation–reduction reactions and plays an essential role in animal metabolism. However, copper contamination can bring about side effects including nausea, dizziness, vomiting, abdominal cramps, convulsions and even death (Paulino *et al.* 2006).

Among traditional methods for the removal of metal ions, adsorption has attracted a broader concern due to its relative high performance and lower cost (Kyzas and Kostoglou 2015). Various adsorbents are suggested and used for this purpose and biosorbents have shown promising results, especially living or dead micro-organisms which are available either as large quantities in nature or extracted as certain waste products from industrial units (Shafaei *et al.* 2007) making them

*Corresponding author, Ph.D., E-mail: ghaee@ut.ac.ir

economical. Among biosorbents, chitosan as a natural polysaccharide has got features such as hydrophilicity, biocompatibility, biodegradability and high affinity for biomacromolecules. It is also a well-known sorbent for heavy metal ions because of amino ($-\text{NH}_2$) and/or hydroxyl ($-\text{OH}$) groups in the chain structure serving as coordination sites (Guibal 2004).

Generally, various forms of chitosan are used for heavy metal ions removal. Chitosan beads are one alternative (Li and Bai 2005, Igberase *et al.* 2014, Li *et al.* 2015). Adsorptive UF separation can improve the retention performance of chitosan beads by rectifying the contact pattern of the fluid containing metal ions with the adsorption sites (Klein 2000). Chitosan powders, flakes or gel beads lack easy reuse capacity and also suffer slow adsorption kinetics (Kaminski and Modrzejewska 1997, Krajewska 2001). The application of chitosan nanocomposites (Wang and Wang 2016), nanoparticles (Yu *et al.* 2013) and hydrogels (Jamnongkan and Singcharoen 2016) are also investigated in some studies although their efficiency and applicability is yet to be investigated. Moreover, some studies have been performed on dynamic systems using fixed-bed columns, but high capital and energy costs of adsorption columns suggest membrane processes to be more favorable for metal ions removal (Guibal 2004). As a result, many studies on metal ion sorption are focused on dense chitosan membranes prepared by evaporation techniques (Cestari *et al.* 2005, Vieira *et al.* 2007, Lopes *et al.* 2003, Baroni *et al.* 2008, Vieira and Beppu 2005, 2006a, b), having low porosity which limits diffusion and flux in continuous processes. Immersion-precipitation (Kamiński and Modrzejewska 1997, 1999) and particulate leaching (Beppu *et al.* 2004, Chao *et al.* 2006, Santos *et al.* 2008, Machado *et al.* 2006, Liao *et al.* 2002, Zeng and Ruckenstein 1996) are also proposed for the preparation of porous and macroporous chitosan membranes. Beppu *et al.* (2004) investigated the effect of porosity (calculated by water sorption) in macroporous chitosan membranes functionalized by histidine and realized that membranes with higher porosity show higher copper adsorption capacities. Chao *et al.* (2006) studied the effect of pore size and porosity of chitosan membranes on the adsorption of dye and copper ions from wastewater and found the strong effect of porosity on the adsorption rate.

In this study, the mechanism of copper ions adsorption on macroporous chitosan membranes was investigated along with XPS study and Isotherm models, rarely reported in the literature. Effect of experimental parameters, i.e. pH, copper initial concentration and temperature on adsorption characteristics are investigated. Langmuir, Freundlich and Langmuir-Freundlich models are fitted to the experimental data in order to illustrate the distribution of copper in the adsorbent and solution. Desorption experiments were also carried out using ethylene diamine tetra acetic acid (EDTA) and NaCl. Moreover, XPS spectroscopy was used to investigate adsorption mechanism.

2. Experimental section

2.1 Materials and methods

Chitosan was purchased from Chitotech with a 90% deacetylation degree. All other chemicals (glutaraldehyde, acetic acid, sodium hydroxide, cupric sulfate, EDTA and NaCl) were of analytical grade used without further purification. Chromatography silica-gel (15-40 μm) was also obtained from Merck Co.

2.2 Membrane preparation

The 7% chitosan solution was poured onto a flat surface upon aeration in order to prepare the porous membrane. A 2 mm slot film applicator is used to adjust the proper membrane thickness.

Immediately after the solution was poured (without solvent evaporation), coagulation was performed in a 4% aqueous solution of sodium hydroxide (non-solvent bath) for 24 h after which the membranes were washed with distilled water.

Preparation of macroporous membranes is performed using a 7% chitosan solution mixed with silica-gel as the porogen at a silica/chitosan weight ratio of 3/1 and poured into a Petri dish and dried at room temperature for 24 h. The membrane was then immersed in an aqueous solution of sodium hydroxide (1 M) for 24 h and then washed with distilled water. Chitosan dissolution in acidic media was decreased through crosslinking treatments. Crosslinking reactions can be performed using specific bi-functional chemicals (glutaraldehyde and epichlorohydrin) which react with specific functional groups. Natural chitosan membranes were heterogeneously crosslinked by immersion in a 0.25% (w/w) aqueous glutaraldehyde (3.0 g of wet chitosan membrane in 50 mL of glutaraldehyde solution) at 25°C for 30 min, followed through washing by distilled water to remove the unreacted glutaraldehyde residues. Finally, the membranes were dried using filter papers.

2.3 Adsorption experiments

Copper ion solutions were prepared by dissolving copper sulfate ($\text{CuSO}_4 \cdot 5\text{H}_2\text{O}$) in deionized water at 50, 100, 200 and 400 ppm concentrations. Batch adsorption experiments were carried out by soaking $2 \times 3 \text{ cm}^2$ of porous and macroporous chitosan membranes in copper solution over 24 h at 20°C and pH = 5 under magnetic stirring, along with measurement of ionic concentration in the solution. This adsorption period is sufficient to reach adsorption equilibrium as verified by kinetic experiments in Section 2.3.2.

To investigate the influence of pH, initial concentration and temperature on adsorption characteristics, experiments were carried out by soaking $2 \times 3 \text{ cm}^2$ of macroporous chitosan membrane in copper solutions at various pH values (adjusted by 0.01 M HCl and NaOH solutions accordingly) and 20°C and various temperatures at the fixed pH = 5 during a 24 h under 150 rpm stirring rate. The amount of adsorbate in the solid phase (q , mg/g) is calculated through the following expression

$$q = (C_0 - C_{eq}) \times \frac{V}{m} \quad (1)$$

Where C_0 and C_{eq} are initial and equilibrium concentrations of metal ion in the liquid phase (mg/L) respectively, V is the solution volume (L) and m is the membrane weight (g).

2.3.1 Copper adsorption isotherms

Adsorption isotherms describe the adsorbate distribution between solid and liquid phases obtained by varying the copper initial concentration (50, 100, 200, and 400 ppm) at different pH values. Also, the correlation of equilibrium data is investigated using Langmuir, Freundlich and Langmuir-Freundlich equations.

2.3.1.1 Langmuir model

Langmuir model is based on the assumption that the adsorbent pore surfaces are homogenous and the interaction forces between the adsorbed molecules are negligible (Shafaei *et al.* 2007)

$$q = \frac{q_{\max} K_L C_{eq}}{1 + K_L C_{eq}} \quad (2)$$

Where, q_{\max} (mg/g) and K_L (L/mg) are the maximum adsorption capacity and Langmuir isotherm constants, respectively.

2.3.1.2 Freundlich model

This isotherm is derived by assuming a heterogeneous surface with non-uniform distribution of heat of adsorption over the surface

$$q = K_F C_{eq}^{b_F} \quad (3)$$

Where K_F ($\text{mg}^{1-b_F} \text{g}^{-1} \text{L}^{b_F}$) and n are Freundlich isotherm constants; q and C_{eq} are adsorption value and equilibrium metal concentration, respectively (Shafaei *et al.* 2007).

2.3.1.3 Langmuir-Freundlich model

This model is a combination of the above mentioned models given as

$$q = \frac{q_{\max} (K_{LF} C_{eq})^{b_{LF}}}{1 + (K_{LF} C_{eq})^{b_{LF}}} \quad (4)$$

Where q_{\max} (mg/g), K_{LF} (L/mg) and b_{LF} are the maximum adsorption capacity and Langmuir-Freundlich isotherm constants.

2.3.2 Adsorption kinetics of copper ion

Adsorption kinetic studies were performed for macroporous chitosan membranes using 50 and 400 ppm initial copper concentrations. To study the sorption kinetics mechanism, certain models are used to investigate the experimental data. The intra-particle diffusion and pseudo-second order kinetic models (Caroni *et al.* 2009) have been utilized to fit the experimental adsorption kinetic results. The intra-particle diffusion equations are expressed as follows

$$q_t = K_D t^{m_D} \quad (5)$$

$$\ln q_t = \ln K_D + m_D \ln t \quad (6)$$

Where K_D ($\text{mg g}^{-1} \text{min}^{-m_D}$) and m_D are the model constants. In this model, sorption process is assumed to occur in three consecutive steps (transport of sorbate to the sorbent external surface, diffusion-controlled transport of sorbate within the sorbent pores and adsorption on the sorbent surface).

If the rate of sorption follows a second-order mechanism, the pseudo-second order equations are expressed as follows (Caroni *et al.* 2009)

$$\frac{dq_t}{dt} = k_2 (q_e - q_t)^2 \quad (7)$$

$$\frac{1}{(q_e - q_t)} = \frac{1}{q_e} + k_2 t \quad (8)$$

$$\frac{1}{q_t} = \frac{1}{k_2 q_e^2} + \frac{1}{q_e} t \quad (9)$$

Where q_e and q_t are the sorption value (mg/g) at equilibrium conditions and time t (min), respectively and k_2 is the rate constant for the pseudo-second order sorption ($\text{g mg}^{-1}\text{min}^{-1}$).

2.4 Desorption experiments

$2 \times 3 \text{ cm}^2$ sections of macroporous chitosan membrane were soaked in copper solution with an initial concentration equal to 400 ppm at pH = 5 and 20°C during a 24 h period under 150 rpm stirring rate. The membranes were washed using distilled water to remove the probable un-adsorbed copper and stirred for 24 h in 30 mL of 10^{-4} M EDTA and 2×10^{-4} M NaCl solutions (Chitosan membranes are soluble in higher concentration of EDTA forming a 1:1 complex with metals). Then the desorbed metal amount was determined as previously described (First cycle: adsorption/desorption) with the second and third cycles just as identical. Copper desorption percentage during each cycle was calculated using (Wan *et al.* 2010)

$$\text{Desorption\%} = \frac{\text{amount of metal desorbed}}{\text{amount of metal absorbed}} \times 100 \quad (10)$$

2.5 Characterization

The membrane surface and cross-section morphologies were analyzed using SEM. Metal ion concentrations were measured using a flame atomic absorption spectrophotometer (Varian AA 240). All reported copper concentrations are the mean value of 3 replicates.

XPS analysis of chitosan membrane before and after adsorption was performed by VG Microtech XR3E2 spectrometer with an Al $K\alpha$ X-ray source (1486.6 eV of photons). SDP 4 XPS international software is used for the analysis of results. The spectra binding energy calibration was performed with the C 1S peak at 285 eV.

3. Results and discussion

3.1 SEM analysis

Figs. 1 and 2 show the SEM micrographs of the top and bottom surfaces and the cross-section of porous and macroporous membranes. The porous membrane prepared by immersion precipitation has a sponge-like structure with tiny pores; however, the macroporous membrane has a porous structure throughout, from the top to the bottom of the membrane with macropores in the range of silica particle size. Also, the macroporous membrane surface has a higher roughness and porosity in comparison.

3.2 Copper adsorption

Table 1 lists the amount of copper adsorption on porous and macroporous membranes at different initial concentrations. In batch experiments, lateral surfaces play an important role in adsorption; so higher surface roughness and macroporosity causes more accessibility of functional groups and metal adsorption due to the reduction of mass transfer resistance. Macropores and higher roughness (from SEM micrographs) in macroporous chitosan membrane results in a higher adsorption capacity compared with the porous counterparts.

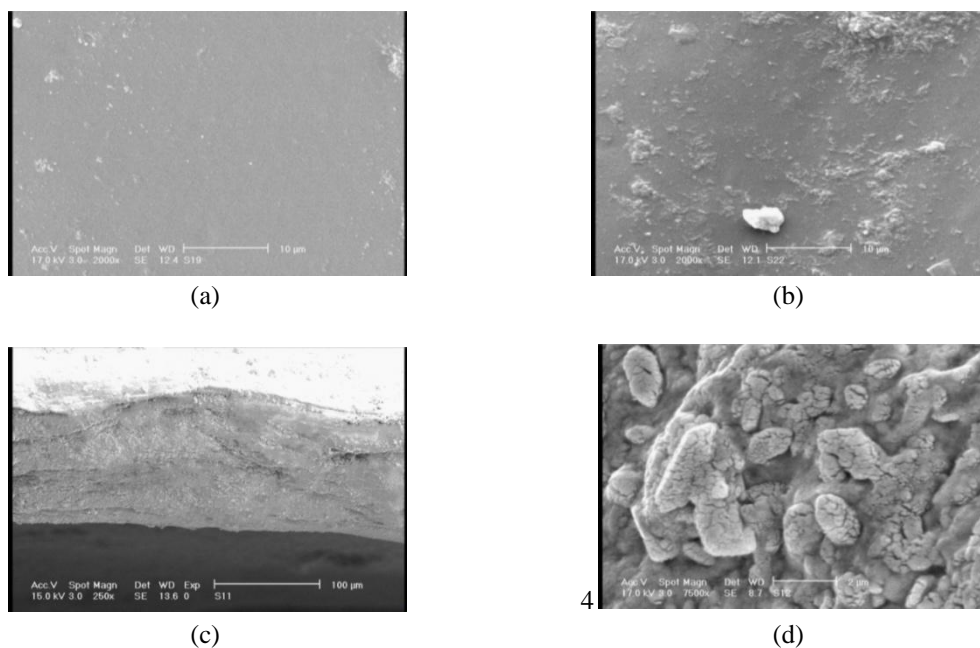


Fig. 1 SEM micrograph of the porous chitosan membrane: (a) Top surface with $\times 2000$ magnification; (b) Bottom surface with $\times 2000$ magnification; (c) Cross-section with $\times 250$ magnification (d) Cross-section with $\times 7500$ magnification

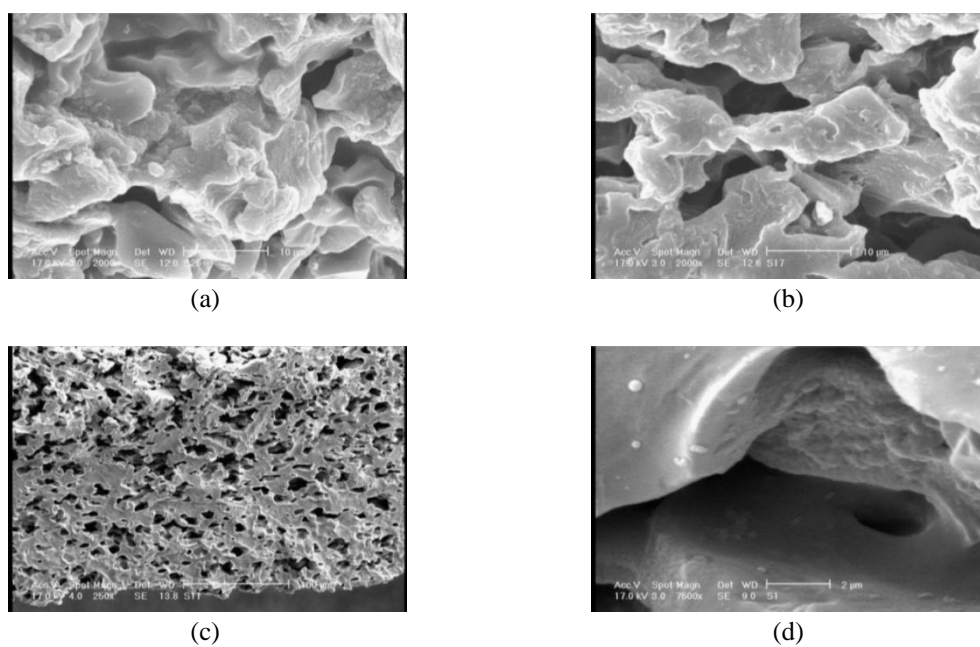


Fig. 2 SEM micrographs of the macroporous chitosan membrane: (a) Top surface with a $\times 2000$ magnification; (b) Bottom surface with a $\times 2000$ magnification; (c) Cross-section with a $\times 250$ magnification; (d) Cross-section with $\times 7500$ magnification

Table 1 The adsorption of copper after 24 h

Initial concentration (ppm)	Porous chitosan (mg/g)	Macroporous chitosan (mg/g)
50	1.74	3.75
100	3.91	7.31
200	5.36	13.87
400	9.84	21.60

3.2.1 Effect of pH

pH values were selected in the range of 2.5-5, which are the lower and upper limits for chitosan dissolution and the precipitation of copper ions, respectively. The results are illustrated in Fig. 3, which shows the enhancement of copper removal with pH increase at different initial concentrations. The lower adsorption in an acidic solution (lower pH) may occur as a result of partial protonation of the active groups and the competition of H⁺ with metal ions for adsorption sites on the macroporous chitosan membrane.

Equilibrium data are correlated by Langmuir, Freundlich and Langmuir-Freundlich equations and the related parameters are presented in Table 2. As can be seen, Langmuir-Freundlich model shows a better fit to the adsorption data which confirm the simultaneous occurrence of chelation and electrostatic adsorption in this process (Gotoh *et al.* 2004, Shafaei *et al.* 2007, Baroni *et al.* 2008, Wan Ngah and Fatinathan 2010a, Cao *et al.* 2010).

3.2.2 Effect of temperature

Effect of temperature on the adsorption of copper ions at different initial concentrations is shown in Fig. 4. The results show that the adsorption capacity is decreased by increasing temperature, implying the exothermic nature of the adsorption process.

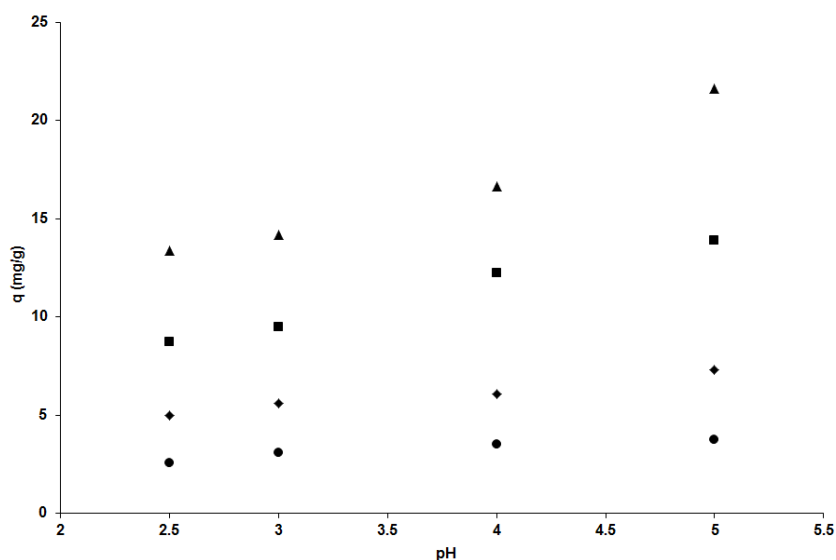


Fig. 3 The effect of pH values on copper adsorption, (●) C0 = 50 ppm, (◆) C0 = 100 ppm, (■) C0 = 200 ppm, (▲) C0 = 400 ppm

Table 2 The constants of isotherm models for copper-chitosan adsorption

Langmuir				
pH	q_{\max} (mg/g)	K_L (L/mg)	R^2	
2.5	9.90099	0.006504	0.978	
3	12.65823	0.005874	0.986	
4	17.85714	0.005602	0.979	
5	20.83333	0.008775	0.972	
Freundlich				
pH	b_F	K_F ($\text{mg}^{1-b_F} \text{g}^{-1} (\text{dm}^3)^{b_F}$)	R^2	
2.5	1.795332	0.275822	0.996	
3	1.666667	0.27036	0.994	
4	1.592357	0.32368	0.999	
5	1.792115	0.608536	0.995	
Langmuir-Freundlich				
pH	q_{\max} (mg/g)	K_{LF} (dm^3/mg)	b_{LF}	R^2
2.5	15.5116	0.0012	0.6407	0.998
3	17.4327	0.0027	0.7885	0.998
4	26.8145	0.0015	0.7276	0.999
5	32.6676	0.0014	0.6023	0.993

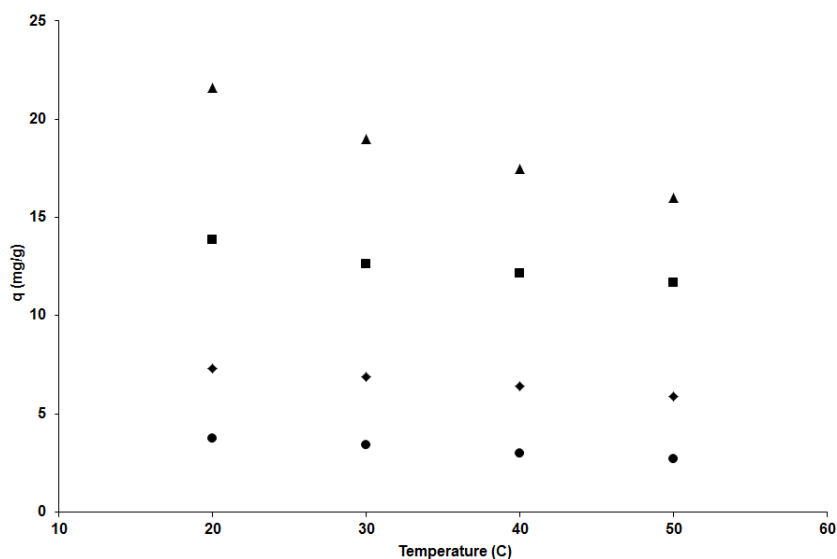


Fig. 4 The effect of temperature on copper adsorption, (●) $C_0 = 50$ ppm, (◆) $C_0 = 100$ ppm, (■) $C_0 = 200$ ppm, (▲) $C_0 = 400$ ppm

Heat of adsorption at constant sorbate values known as isosteric heat of adsorption (ΔH_x) is calculated using Clausius–Clapeyron equation. (Monier *et al.* 2010)

$$\Delta H_x = R \left[\frac{d(\ln C_{eq})}{d\left(\frac{1}{T}\right)} \right] \tag{11}$$

Where R denotes the molar gas constant (8.314 J/mol K). For this purpose, the equilibrium concentration (C_{eq}) is obtained from the adsorption data at different temperatures (K). ΔH_x is calculated from the slope of the $\ln(C_{eq})$ vs. $1/T$. The calculated enthalpy changes are -3.170 ($R^2 =$

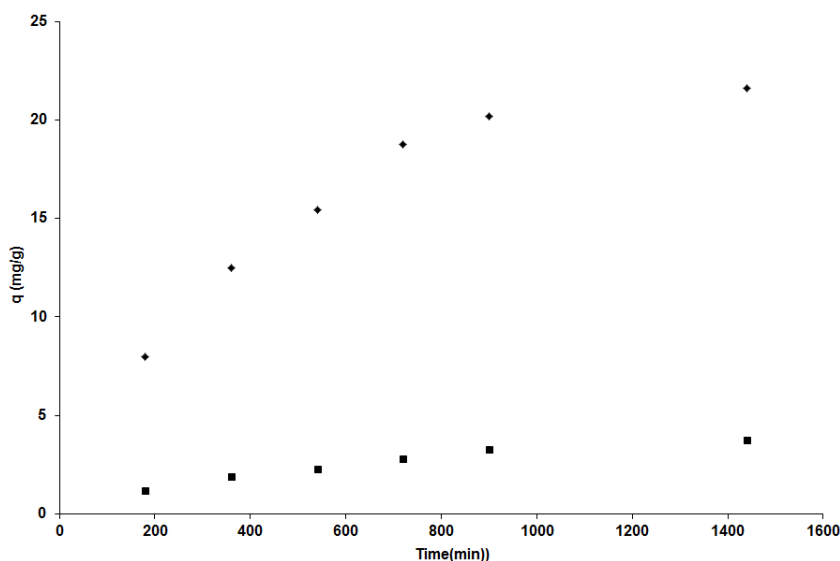


Fig. 5 Copper adsorption for (■) $C_0 = 50$ ppm, (◆) $C_0 = 400$ ppm at different times

Table 3 Kinetic model constants for copper-chitosan adsorption

Intra-particle model			
Copper initial concentration (ppm)	K_D (mg g ⁻¹ min ^{-m})	m_D	R^2
50	0.0627	0.572	0.985
400	0.639	0.5004	0.955
Pseudo-second order model			
Copper initial concentration (ppm)	K_2 (g mg ⁻¹ min ⁻¹)	q_e (mg/g)	R^2
50	0.0055	5.64	0.996
400	0.000075	29.15	0.993

Table 4 Desorption percent of copper ions during adsorption/desorption cycles

Cycle No.	EDTA	NaCl
1	84.96	66.71
2	73.23	54.89
3	61.58	40.16

0.9981), - 3.784 ($R^2 = 0.9988$), - 4.366 ($R^2 = 0.997$) and - 4.647 ($R^2 = 0.9989$) kJ/mol for 50, 100, 200 and 400 ppm initial concentrations, respectively.

3.2.3 Effect of initial concentration

Figs. 3 and 4 show that the copper adsorption amount is increased by increasing the metal ion initial concentration at various pH values and temperatures, which can be attributed to the mass transfer effects and concentration gradient driving force directly proportional to initial concentrations.

3.2.4 Effect of contact time

Fig. 5 shows the effect of agitation time on copper adsorption. The results show that the adsorption is increased by increasing the agitation time and reaches equilibrium conditions gradually during a 24 h period. During the experiment, copper concentration and as a result mass transfer driving force is decreased and hence the adsorption rate decreases considerably, while higher adsorption rates are examined at the beginning. Also, kinetic models are fitted to experimental data. The constants for the intra-particle diffusion and pseudo-second order model are presented in Table 3. It is obvious that the adsorption of copper ions, are fitted well to a pseudo second-order kinetic model which proves that chelation as the dominant mechanism (Cestari *et al.* 2005).

3.3 Desorption experiments

Desorption studies contribute greatly to the elucidation of the nature of adsorption process and also metal ion recovery as well as adsorbent regeneration. Table 4 shows copper desorption percentage per cycle for EDTA and NaCl. As shown in Table 3, the desorption ratio of ions using EDTA and NaCl were 84.96 and 66.71 during the first cycle, respectively. For second and third cycles, these values decreased probably due to the driving force reduction. From the results, EDTA was shown to be a better eluant than NaCl. The results confirm chelation as the dominant sorption mechanism.

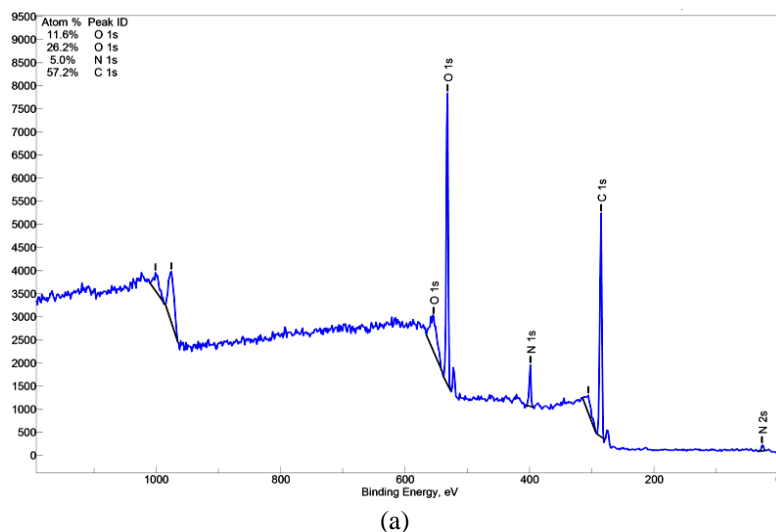
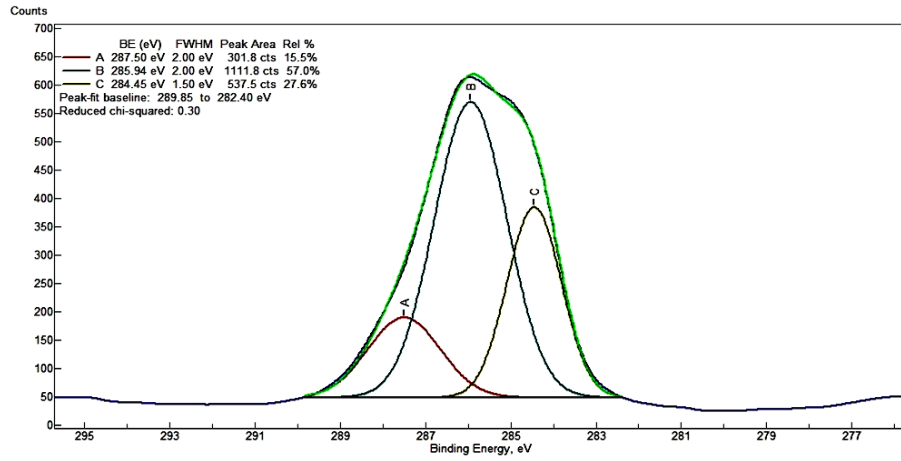
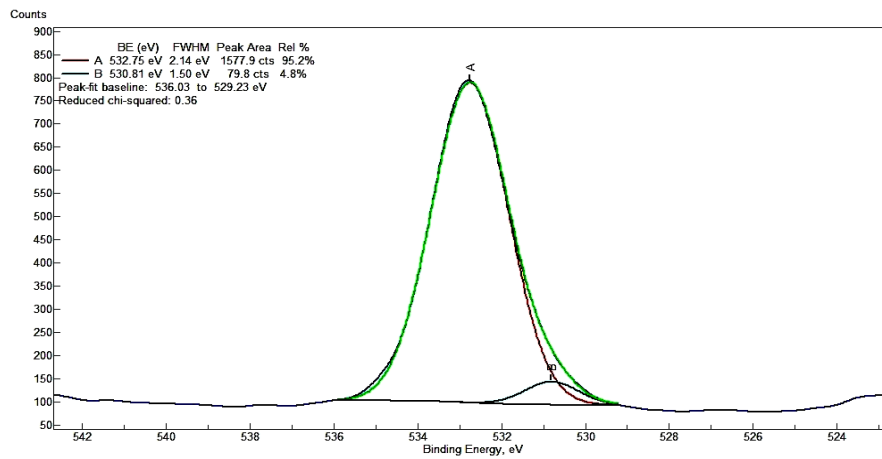


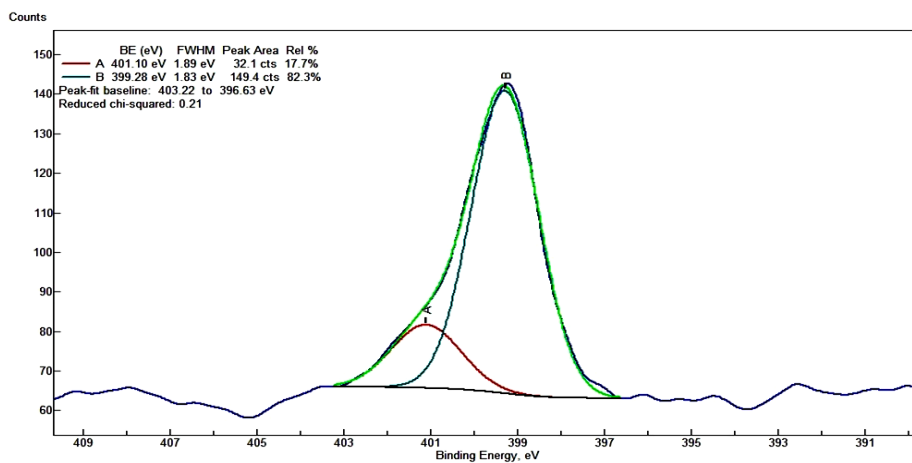
Fig. 6 The XPS spectra for chitosan membrane before adsorption for: (a) all compositions; (b) C1S; (c) O1S; (d) N1S



(b)



(c)



(d)

Fig. 6 Continued

3.4 Adsorption mechanism

XPS spectra have been widely used to identify the existence of a particular element and also distinguish various forms of the same element in a material. Figs. 6 and 7 show the XPS spectra of chitosan membrane before and after copper sorption. The C1s spectra of the chitosan membrane before copper adsorption are shown in Fig. 6(b). There are 3 peaks at 284.38, 285.94 and 287.49 eV assigned to C-C groups, C-O bonding and C = O groups existing in the residual chitin-like rings. The O1s spectra (Fig. 6(c)) show two peaks at 530.81 and 532.72 eV due to C-OH and C-O bonds. The N1s spectra show two peaks at 399.28 and 401.01 eV attributed to N atom in the R-NH₂ group and R-NH₃⁺ (Kang *et al.* 2010, Jin and Bai 2002, Hasan *et al.* 2008).

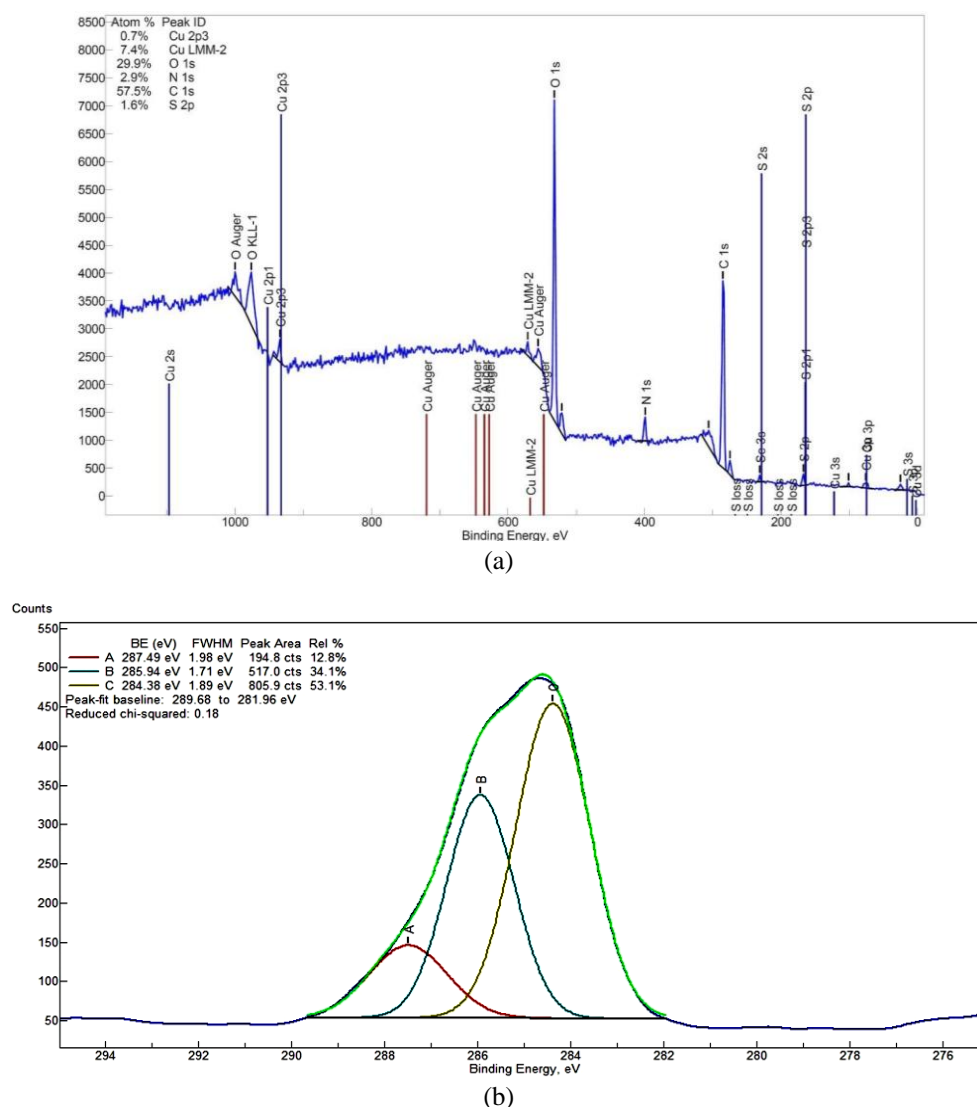


Fig. 7 XPS spectra for chitosan membrane after adsorption for: (a) all compositions; (b) C1s; (c) O1s; (d) N1s; (e) Cu; (f) S

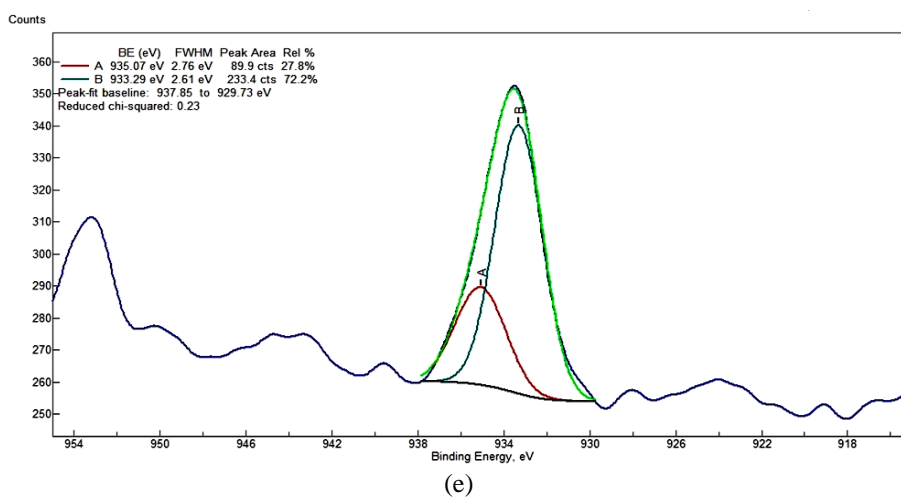
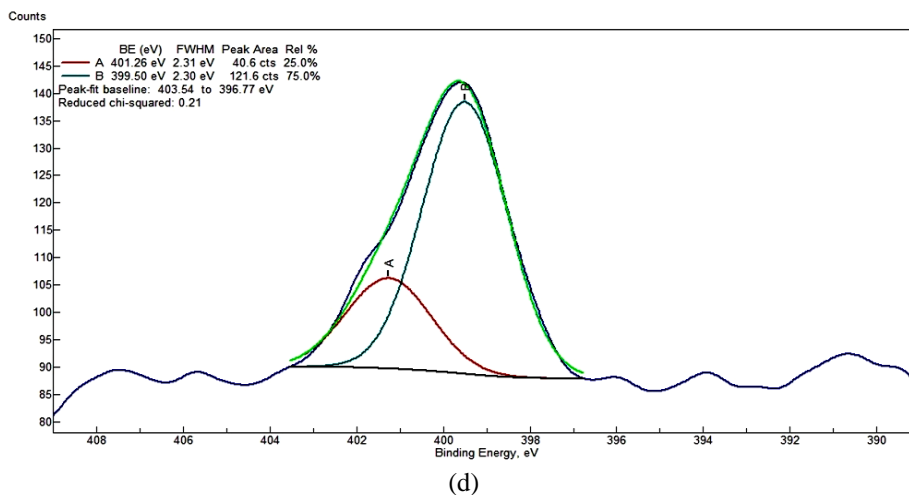
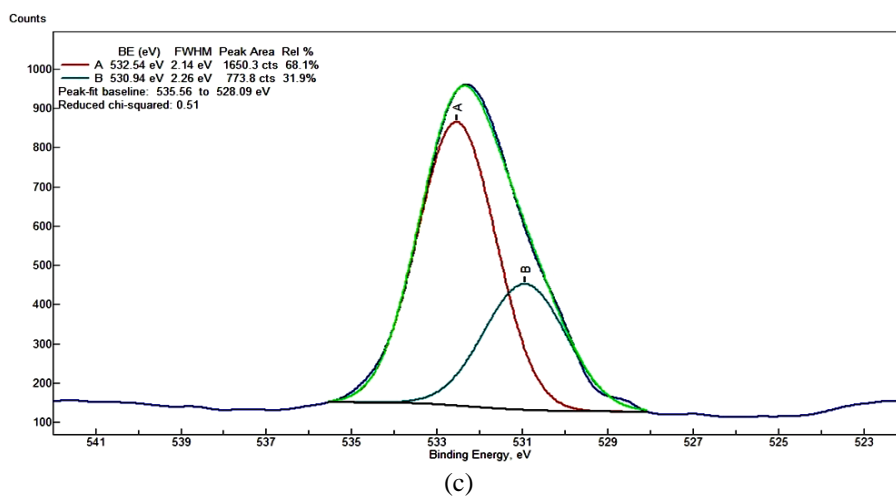


Fig. 7 Continued

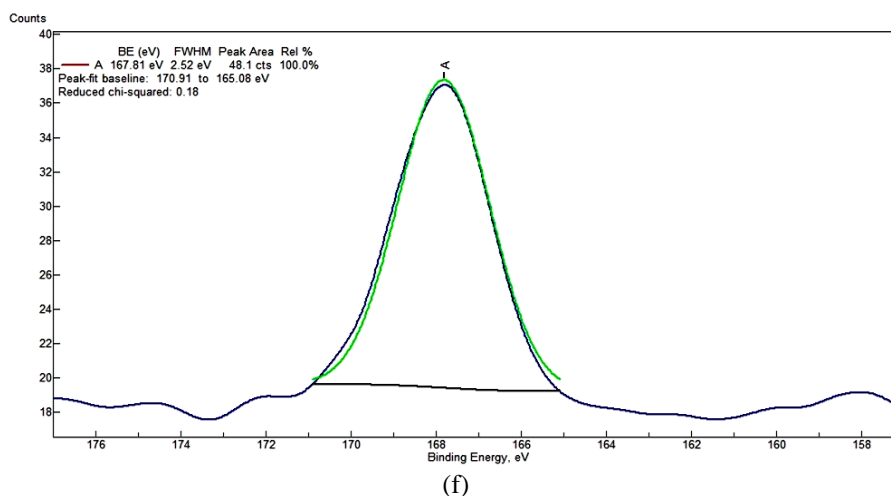


Fig. 7 Continued

No difference is distinguished between C1s (Fig. 7(b)) and O1s (Fig. 7(c)) spectra of chitosan membrane before and after adsorption. The data indicate that carbon and oxygen containing functional groups had limited participation in metal binding reaction. By comparing N1s spectra (Fig. 7(d)) before and after adsorption, one can conclude that some R-NH₂ bonds are shifted to 401.26 eV, which means that some N atoms exist in a more oxidized state due to copper adsorption (Kang *et al.* 2010, Jin and Bai 2002, Hasan *et al.* 2008).

Fig. 7(e) shows the XPS spectrum of Cu 2p_{3/2} core regions of chitosan membrane upon adsorption. Two peaks are observed at 933.29 eV and 935.07 eV which confirm the existence of a 3d⁹ shell of Cu²⁺. The CuLMM Auger peak appeared at 570 eV (Fig. 7(a)). The Auger parameter (α'_0) is calculated using the following equation (Vieira *et al.* 2011)

$$\alpha'_0 = KE_{CuLMM} - \frac{KE_{Cu2p3/2}}{2} + 1253.6 \quad (12)$$

Where KE_{CuLMM} and $KE_{Cu2p3/2}$ are the kinetic energy of the CuLMM Auger electron and Cu 2p_{3/2} photoelectron, respectively. α'_0 is calculated as 1849.9 eV which confirms the formation of Cu₂O. Fig. 7(f) shows the XPS spectra for sulfur compounds. The existence of sulfur in the spectra confirms simultaneous occurrence of electrostatic and chelation adsorption mechanisms.

4. Conclusions

Porous and macroporous chitosan membranes were prepared for heavy metal adsorption. The membrane surface and cross-section morphologies were investigated using SEM micrographs. The macroporous chitosan membrane had an asymmetric porous structure and more rough both on top and bottom surfaces. SEM micrographs of porous chitosan membrane showed a sponge-like structure. It was observed that macroporous chitosan membranes had a higher adsorption capacity, which may be attributed to higher roughness and lower mass transfer resistance due to pore sizes. Effect of various parameters such as pH, initial metal concentration and temperature on adsorption was studied in this study. The adsorption value is increased with pH and initial metal concentration

while being decreased by increasing the temperature. XPS results confirm the mutual effect of chelation and electrostatic effects on adsorption just as Langmuir-Freundlich Isotherms does.

References

- Baroni, P., Vieira, R., Meneghetti, E., Silva, M. and Beppu, M. (2008), "Evaluation of batch adsorption of chromium ions on natural and cross-linked chitosan membranes", *J. Hazard. Mater.*, **152**(3), 1155-1163.
- Beppu, M., Arruda, E., Vieira, R. and Santos, N. (2004), "Adsorption of Cu (II) on porous chitosan membranes functionalized with histidine", *J. Membrane Sci.*, **240**(1-2), 227-235.
- Cao, J., Tan, Y., Che, Y. and Xin, H. (2010), "Novel complex gel beads composed of hydrolyzed polyacrylamide and chitosan: An effective adsorbent for the removal of heavy metal from aqueous solution", *Bioresource Techno.*, **101**(7), 2558-2561.
- Caroni, A., De Lima, C., Pereira, M. and Fonseca, J. (2009), "The kinetics of adsorption of tetracycline on chitosan particles", *J. Colloid Interf. Sci.*, **340**(2), 182-191.
- Cestari, A., Vieira, E., Matos, J. and Anjos, F. (2005), "Determination of kinetic parameters of Cu (II) interaction with chemically modified thin chitosan membranes", *J. Colloid Interf. Sci.*, **285**(1), 288-295.
- Chao, A., Yu, S. and Chuang, G. (2006), "Using NaCl particles as porogen to prepare a highly adsorbent chitosan membrane", *J. Membrane Sci.*, **280**(1-2), 163-174.
- Gotoh, T., Matsushima, K. and Kikuchi, K.I. (2004), "Preparation of alginate-chitosan hybrid gel beads and adsorption of divalent metal ions", *Chemosphere*, **55**(1), 135-140.
- Guibal, E. (2004), "Interactions of metal ions with chitosan-based sorbents: A review", *Sep. Purifi. Technol.*, **38**(1), 43-74.
- Hasan, S., Ghosh, T., Viswanath, D. and Boddu, V. (2008), "Dispersion of chitosan on perlite for enhancement of copper (II) adsorption capacity", *J. Hazard. Mater.*, **152**(2), 826-837.
- Igberase, E., Osifo, P. and Ofomaja, A. (2014), "The adsorption of copper (II) ions by polyaniline graft chitosan beads from aqueous solution: Equilibrium, kinetic and desorption studies", *J. Environ. Chem. Eng.*, **2**(1), 362-369.
- Jin, L. and Bai, R. (2002), "Mechanisms of lead adsorption on chitosan/PVA hydrogel beads", *Langmuir*, **18**(25), 9765-9770.
- Jamnongkan, T. and Singcharoen, K. (2016), "Towards novel adsorbents: the ratio of PVA/chitosan blended hydrogels on the copper (II) ion adsorption", *Energy Procedia*, **89**, 299-306.
- Kang, J., Liu, H., Zheng, Y., Qu, J. and Chen, J. (2010), "Systematic study of synergistic and antagonistic effects on adsorption of tetracycline and copper onto a chitosan", *J. Colloid Interf. Sci.*, **344**(1), 117-125.
- Kamiński, W. and Modrzejewska, Z. (1997), "Application of chitosan membranes in separation of heavy metal ions", *Sep. Sci. Technol.*, **32**(16), 2659-2668.
- Kamiński, W. and Modrzejewska, Z. (1999), "Separation of Cr (VI) on chitosan membranes", *Ind. Eng. Chem. Res.*, **38**(12), 4946-4950.
- Klein, E. (2000), "Affinity membranes: A 10-year review", *J. Membr. Sci.*, **179**(1-2), 1-27.
- Krajewska, B. (2001), "Diffusion of metal ions through gel chitosan membranes", *React. Funct. Polym.*, **47**(1), 37-47.
- Kyzas, G.Z. and Kostoglou, M. (2015), "Swelling-adsorption interactions during mercury and nickel ions removal by chitosan derivatives", *Sep. Purif. Technol.*, **149**, 92-102
- Li, N. and Bai, R. (2005), "Copper adsorption on chitosan-cellulose hydrogel beads: Behaviours and mechanisms", *Sep. Purifi. Technol.*, **42**(3), 237-247.
- Li, L., Li, Y., Cao, L. and Yang, C. (2015), "Enhanced chromium (VI) adsorption using nanosized chitosan fibers tailored by electrospinning", *Carbohydr. Polym.*, **125**, 206-213
- Liao, C., Chen, C., Chen, J., Chiang, S., Lin, Y. and Chang, K. (2002), "Fabrication of porous biodegradable polymer scaffolds using a solvent merging/particulate leaching method", *J. Biomed. Mater. Res.*, **59**(4), 676-681.
- Lopes, E., Anjos, F., Vieira, E. and Cestari, A. (2003), "An alternative Avrami equation to evaluate kinetic

- parameters of the interaction of Hg (II) with thin chitosan membranes”, *J. Colloid Interf. Sci.*, **263**(2), 542-547.
- Machado, R., Arruda, E., Santana, C. and Bueno, S. (2006), “Evaluation of a chitosan membrane for removal of endotoxin from human IgG solutions”, *Process Biochem.*, **41**(11), 2252-2257.
- Monier, M., Wei, Y. and Sarhan, A. (2010), “Preparation and characterization of magnetic chelating resin based on chitosan for adsorption of Cu (II), Co (II) and Ni (II) ions”, *React. Funct. Polym.*, **70**(4), 257-266.
- Paulino, A., Minasse, F., Guilherme, M., Reis, A., Muniz, E. and Nozaki, J. (2006), “Novel adsorbent based on silkworm chrysalides for removal of heavy metals from wastewaters”, *J. Colloid Interf. Sci.*, **301**(2), 479-487.
- Santos, D., Neto, C., Fonseca, J. and Pereira, M. (2008), “Chitosan macroporous asymmetric membranes: Preparation, characterization and transport of drugs”, *J. Membrane Sci.*, **325**(1), 362-370.
- Shafaei, A., Zokaee Ashtiani, F. and Kaghazchi, T. (2007), “Equilibrium studies of the sorption of Hg (II) ions onto chitosan”, *Chem. Eng. J.*, **133**(1-3), 311-316.
- Vieira, R. and Beppu, M. (2005), “Mercury ion recovery using natural and cross-linked chitosan membranes”, *Adsorption*, **11**(1), 731-736.
- Vieira, R. and Beppu, M. (2006a), “Dynamic and static adsorption and desorption of Hg (II) ions on chitosan membranes and spheres”, *Water Res.*, **40**(8), 1726-1734.
- Vieira, R. and Beppu, M. (2006b), “Interaction of natural and cross-linked chitosan membranes with Hg (II) ions”, *Colloid. Surf. A*, **279**(1-3), 196-207.
- Vieira, R., Guibal, E., Silva, E. and Beppu, M. (2007), “Adsorption and desorption of binary mixtures of copper and mercury ions on natural and cross-linked chitosan membranes”, *Adsorption*, **13**(5), 603-611.
- Vieira, R., Oliveira, M., Guibal, E., Castellón, E. and Beppu, M. (2011), “Copper, mercury and chromium adsorption on natural and cross-linked chitosan films: An XPS investigation of mechanism”, *Colloid. Surf. A*, **374**, 108-114.
- Wan, M., Kan, C., Rogel, B. and Dalida, M. (2010), “Adsorption of Copper (II) and Lead (II) ions from aqueous solution on chitosan-coated sand”, *Carbohydr. Polym.*, **80**(3), 891-899.
- Wan Ngah, W.S. and Fatinathan, S. (2010a), “Adsorption characterization of Pb (II) and Cu(II) ions onto chitosan-tripolyphosphate beads: Kinetic, equilibrium and thermodynamic studies”, *J. Environ. Manag.*, **91**(4), 958-969.
- Wan Ngah, W.S. and Fatinathan, S. (2010b), “Pb (II) biosorption using chitosan and chitosan derivatives beads: Equilibrium, ion exchange and mechanism studies”, *J. Environ. Sci.*, **22**(3), 338-346.
- Wang, X. and Wang, Ch. (2016), “Chitosan-poly (vinyl alcohol)/attapulgitite nanocomposites for copper (II) ions removal: pH dependence and adsorption mechanisms”, *Colloid. Surf. A: Physicochem. Eng. Aspects*, **500**, 186-194.
- Yu, K., Ho, J., McCandlish, E., Buckley, B., Patel, R., Li, Zh. and Shapley, N.C. (2013), “Copper ion adsorption by chitosan nanoparticles and alginate micro-particles for water purification applications”, *Colloid. Surf. A: Physicochem. Eng. Aspects*, **425**, 31-41.
- Zeng, X. and Ruckenstein, E. (1996), “Control of pore sizes in macroporous chitosan and chitin membranes”, *Ind. Eng. Chem. Res.*, **35**(11), 4169-4175.

Nomenclature

b_F	Freundlich isotherm constant
b_{LF}	Langmuir-Freundlich isotherm constant
C_0	Initial concentration of metal ion in the liquid phase (mg/L)
C_{eq}	Equilibrium concentration of metal ion in the liquid phase (mg/L)
k_2	Rate constant of pseudo-second order sorption ($\text{g mg}^{-1} \text{min}^{-1}$)
K_D	Intra particle diffusion constant ($\text{mg g}^{-1} \text{min}^{-m}$)
K_L	Langmuir isotherm constant (L/mg)
K_F	Freundlich isotherm constant ($\text{mg}^{1-b_F} \text{g}^{-1} (\text{dm}^3)^{b_F}$)
K_{LF}	Langmuir-Freundlich isotherm constant (L/mg)
m	Amount of chitosan membrane (g)
m_D	Intra particle diffusion constant
q	Adsorption amount (mg/g)
q_e	Adsorption amount at equilibrium (pseudo-second order equation constant) (mg/g)
q_{\max}	Maximum adsorption capacity (Langmuir isotherm constant) (mg/g)
q_t	Sorption amount at time t (mg/g)
R	Molar gas constant (8.314 J/mol K)
T	Temperature (K)
t	Time (min)
V	Volume of the solution (L)
$H_x\Delta$	Isosteric heat of adsorption (kJ/mol)